SAN FRANCISCO ESTUARY & WATERSHED SCIENCE
Sponsored by the Delta Science Program and the UC Davis Muir Institute

RESEARCH

Effects of Tidally Varying River Flow on Entrainment of Juvenile Salmon into Sutter and Steamboat Sloughs

Jason G. Romine[1,3], Russell W. Perry*[1], Paul R. Stumpner[2], Aaron R. Blake[2], Jon R. Burau[2]

ABSTRACT

Survival of juvenile salmonids in the Sacramento–San Joaquin Delta (Delta) varies by migration route, and thus the proportion of fish that use each route affects overall survival through the Delta. Understanding factors that drive routing at channel junctions along the Sacramento River is therefore critical to devising management strategies that maximize survival. Here, we examine entrainment of acoustically tagged juvenile Chinook Salmon into Sutter and Steamboat sloughs from the Sacramento River. Because these sloughs divert fish away from the downstream entrances of the Delta Cross Channel and Georgiana Slough (where fish access the low-survival region of the interior Delta), management actions to increase fish entrainment into Sutter and Steamboat sloughs are being investigated to increase through-Delta survival. Previous studies suggest that fish generally "go with the flow"—as net flow into a divergence increases, the proportion of fish that enter that divergence correspondingly increases. However, complex tidal hydrodynamics at sub-daily time-scales may be decoupled from net flow. Therefore, we modeled routing of acoustic tagged juvenile salmon as a function of tidally varying hydrodynamic data, which was collected using temporary gaging stations deployed between March and May of 2014. Our results indicate that discharge, the proportion of flow that entered the slough, and the rate of change of flow were good predictors of an individual's probability of being entrained. In addition, interactions between discharge and the proportion of flow revealed a non-linear relationship between flow and entrainment probability. We found that the highest proportions of fish are likely to be entrained into Steamboat Slough and Sutter Slough on the ascending and descending limbs of the tidal cycle, when flow changes from positive to negative. Our findings characterize how patterns of entrainment vary with tidal flow fluctuations, providing information critical for understanding the potential effect of management

SFEWS Volume 19 | Issue 2 | Article 4

https://doi.org/10.15447/sfews.2021v19iss2art4

* Corresponding author: *rperry@usgs.gov*

1 Western Fisheries Research Center
US Geological Survey
Cook, WA 98605 USA

2 California Water Science Center
US Geological Survey
Sacramento, CA 95819 USA

3 Current address: Mid-Columbia Fish and Wildlife Conservation Office
Yakima Basin Program
US Fish and Wildlife Service
Yakima, WA 98903 USA

actions (e.g., fish guidance structures) to modify routing probabilities at this location.

KEY WORDS

Telemetry, juvenile salmon, migration routing, survival

INTRODUCTION

The Sacramento–San Joaquin River Delta (hereafter referred to as "the Delta") is a complex series of channels and embayments in west central California of the United States. The Delta has undergone drastic transformation through construction of dikes, levees, reclaimed land, dredged canals and cuts, and water export projects (Nichols et al. 1986). The loss of habitat coupled with introduction of non-native piscivorous fishes has led to the decline of several salmonid stocks that utilize the Delta (Lindley 2009; National Marine Fisheries Service 2014). The physical complexity of the Delta poses significant challenges for understanding how juvenile salmon negotiate the complex channel network and survive in different migration routes. Yet such information is critical for understanding how water-management actions, such as operation of water diversions, influence survival of juvenile salmon.

Through-Delta survival of juvenile Chinook Salmon that emigrate from the Sacramento River ranges from 10% to 80%, depending on river flow and migration route (Perry et al. 2018). The Delta can be broken down into four primary routes: (1) Sacramento River, (2) Steamboat and Sutter sloughs, (3) Georgiana Slough, and (4) Delta Cross Channel (DCC). Fish that remain in the Sacramento River consistently have the highest survival (Perry et al. 2010, 2013, 2018). However, fish that enter the interior Delta—the region to the south of the Sacramento River (Figure 1)—have the lowest survival among all routes and survive at less than half the rate of fish in the Sacramento River, likely as a result of longer migration times and exposure to non-native predators (Newman and Brandes 2010; Perry et al. 2018). On average, fish that migrate through Steamboat and Sutter sloughs exhibit survival similar to fish that remain in the Sacramento River at high flows but have lower survival at low flows (Perry et al. 2018).

Because of differences in survival among migration routes, the proportion of fish that use each route affects the total survival of the population. Therefore, understanding the drivers behind fish routing in the Delta is imperative to inform management actions that help in the recovery of imperiled salmonid populations in the Central Valley. For example, Perry et al. (2013) found that total survival through the Delta could be increased by up to 7 percentage points by eliminating entrainment into Georgiana Slough and the DCC. These findings led to investigation of management actions to reduce entrainment into the DCC (Plumb et al. 2016) and Georgiana Slough (Perry et al. 2014).

Both physical and non-physical barriers have been tested at the entrance to Georgiana Slough divergence (Perry et al. 2014; Romine et al. 2016). A non-physical barrier was able to reduce entrainment to the interior Delta through Georgiana Slough (Perry et al. 2014), but a floating fish-guidance structure reduced entrainment to a lesser extent (Romine et al. 2016). Research and engineering solutions to minimize entrainment have focused on the Georgiana Slough divergence, the DCC divergence, and the Old River divergence in the San Joaquin River (Buchanan et al. 2013; SJRG 2013). However, there has been little focus on understanding fish routing dynamics at other primary river junctions in the Delta, such as Sutter and Steamboat sloughs.

Sutter and Steamboat sloughs diverge from the Sacramento about 10 km upstream from the DCC and Georgiana slough, and represent the first major junction that juvenile salmon encounter as they enter the Delta from the Sacramento River (Figure 1). Because Sutter and Steamboat sloughs are upstream of the entrance to the interior Delta via the DCC and Georgiana Slough (Figure 1), juvenile salmon that enter Sutter and Steamboat sloughs avoid entrainment into the interior Delta where survival is low. Thus, management actions to increase entrainment could increase overall

survival by reducing the proportion of fish that enter the interior Delta. However, analytical work by Perry et al. (2013) revealed that the sensitivity of overall survival to entrainment into Sutter and Steamboat sloughs depended not only on the proportion of fish that entered these routes but also on the difference in survival between alternative routes. Based on these findings, Sutter and Steamboat sloughs have received increasing attention by water management agencies as a potential location where fish-guidance solutions could be applied to increase survival of juvenile salmonids that migrate through the Delta. Although past work has estimated that 20% to 40% of juvenile salmon enter Sutter and Steamboat sloughs (Perry et al. 2013, 2018), there is little understanding about the effect of fine-scale tidal hydrodynamics on routing, which can influence the efficacy of management actions to modify routing (e.g., Perry et al. 2014, 2015).

In this paper, we examine juvenile salmonid entrainment into Sutter Slough and Steamboat Slough using data from a large telemetry study conducted during the spring of 2014, which had the primary objective of evaluating a floating fish-guidance structure at Georgiana Slough (Romine et al. 2016). During this study, the US Geological Survey (USGS) deployed temporary gauging stations to measure discharge of the Sacramento River in the vicinity of Sutter and Steamboat sloughs. The availability of these flow data in 2014 provided a rare opportunity to better understand how the routing of juvenile salmon related to flow dynamics at this junction, which provides information critical to understanding fish entrainment patterns.

METHODS

Study Area

Sutter Slough diverges from the Sacramento River 40 river km downstream of the city of Sacramento, and Steamboat Slough is located 2.5 km downstream of Sutter Slough (Figure 1). Tidal flow dynamics at this junction are complex when river inflow to the Delta is sufficiently low (flow at Freeport is less than 210 $m^3 s^{-1}$) to cause reverse flows in Sutter Slough, Steamboat Slough, and the Sacramento River below Steamboat Slough. During the transition from the ebb to flood tide, Steamboat Slough reverses and flows upstream into the Sacramento River. As the ebb-to-flood transition continues, the Sacramento River begins to reverse, and finally, flow in Sutter Slough begins to reverse. Conversely, on the flood-to-ebb transition, these channels cease flow reversals in the opposite order; that is, flow reversals stop first in Sutter Slough, followed by the Sacramento River and Steamboat Slough (See Appendix A on page 15 to view a static image and access an animation of flow dynamics). In general, when flow at Freeport is between 12 and 407 $m^3 s^{-1}$ and flow below Steamboat Slough in the Sacramento River is between 0 and 224 $m^3 s^{-1}$, Steamboat Slough can reverse into the Sacramento River while both the Sacramento River and Sutter Slough maintain downstream flows. Tidal dynamics dictate the strength and duration of reversals. Finally, at high inflow (flow greater than 200 $m^3 s^{-1}$ at Freeport) tidal forcing is dampened, and reverse flows cease altogether (Appendix A).

Fish Tagging

The study used juvenile late-fall run Chinook Salmon (*Oncorhynchus tshawytscha*) reared at the US Fish and Wildlife Service (USFWS) Coleman National Fish Hatchery located in Anderson, California, US Chinook Salmon were tagged and released at the Tower Bridge in the city of Sacramento. We used two types of acoustic tags in the study: the model 900-LD (HTI, Seattle, Washington, US) acoustic transmitters that had a dry weight of 0.96 grams, and the V5 (VEMCO, Bedford, Nova Scotia, Canada) acoustic transmitter that had a dry weight of 0.65 grams. We selected juvenile Chinook Salmon within the size range of 105 to 213 mm fork length (approximately 20 to 40 grams) for tagging. Fish handling, holding, and tag implantation procedures followed the protocols outlined in Liedtke and Wargo–Rub (2012) and Liedtke et al. (2012). We released fish in groups of 8 to 13 individuals every 3 hours from March 1, 2014 to April 15, 2014, for a total release of 4,635 tagged fish.

https://doi.org/10.15447/sfews.2021v19iss2art4

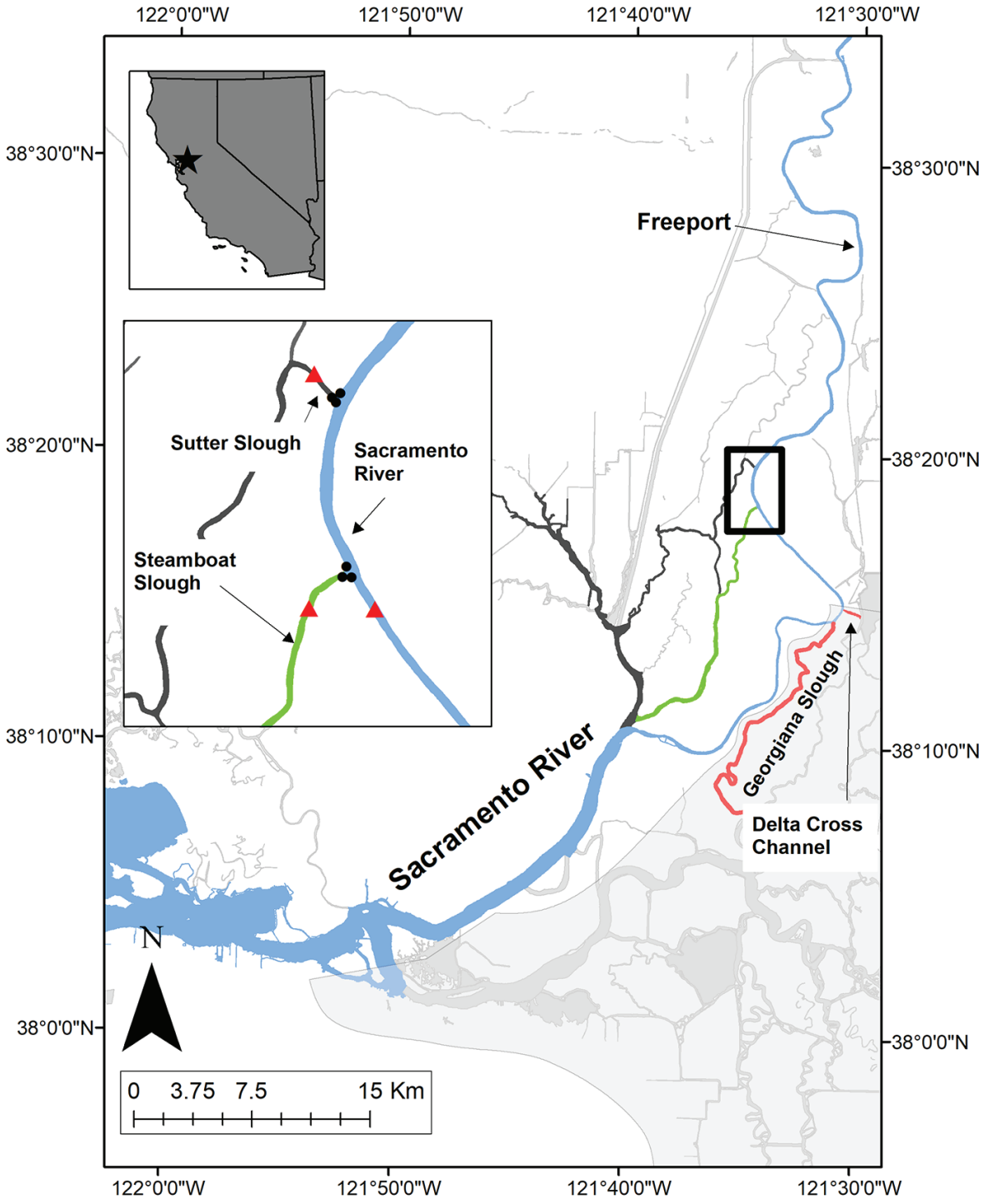

Figure 1 The Sacramento–San Joaquin Delta showing the junction of Sutter and Steamboat sloughs with the Sacramento River (*black box*), the junction of the Delta Cross Channel and Georgiana Slough with the Sacramento River (*asterisk*), and the interior Delta (*the gray region south of the Sacramento River*). The inset map shows the three routes that compose the junction of the Sacramento River with Sutter and Steamboat sloughs. *Blue* indicates the Sacramento River, *green* indicates Steamboat Slough, and *dark gray* indicates Sutter Slough. *Red triangles* indicate the locations of the telemetry equipment used to determine fish route selection, and the *black points* indicate the location of the temporary flow stations. Georgiana Slough and the Delta Cross Channel are identified in *red*. (NAD1983)

Data Collection

We collected telemetry data from acoustically tagged juvenile Chinook Salmon moving into and past Sutter Slough and Steamboat Slough during the spring of 2014. Since two tag types were used, we placed both HTI and VEMCO equipment at the junction. We used six hydrophones (HTI Model 590) coupled with receivers (HTI Model 290) and six VEMCO VR2W receivers (180 kHz) to monitor fish entrainment in the study area. We placed hydrophones (HTI) and receivers (VEMCO) within each of the three possible routes (Sutter Slough, Steamboat Slough, and Sacramento River), just far enough downstream to prevent the detection range of receivers to overlap with unintended routes.

We measured discharge at the junction by six temporary flow stations. Three were located near Sutter Slough (above, inside, and below), and three were located near Steamboat Slough (above, inside and below; Figure 1). We deployed Side-Looker Acoustic Doppler Current Profilers (SL-ADCPs) near the water surface, to measure near-surface water velocities. We developed stage-area and index velocity ratings from down-looking ADCP measurements that occurred over one tidal cycle. We used these ratings to estimate a time-series of discharge using the index–velocity method (Ruhl and Simpson 2005). The flow stations provided a detailed time-series of 15-minute discharge data to quantify the flow dynamics when each tagged fish passed through the river junction.

Route Entrainment Analysis

Route entrainment—the probability that a fish enters one of the three alternative migration routes (Sutter Slough, Steamboat Slough, Sacramento River)—was modeled as a multivariate Bernoulli random variable with the probability distribution

$$\mathrm{P}\left(Y_{ij}=y_{ij}\right)=\pi_{i\mathrm{SUT}}^{y_{i\mathrm{SUT}}}\pi_{i\mathrm{STM}}^{y_{i\mathrm{STM}}}\pi_{i\mathrm{SAC}}^{y_{i\mathrm{SAC}}} \quad (1)$$

where

$\pi_{i,SUT}$ = probability the ith fish ($i = 1, \ldots, n$) entered Sutter Slough,

$\pi_{i,STM}$ = probability the ith fish entered Steamboat Slough,

$\pi_{i,\mathrm{SAC}} = 1 - \pi_{i\mathrm{SUT}} - \pi_{i\mathrm{STM}}$ = probability the ith fish remained in the Sacramento River, and

$$y_{ij} = \begin{cases} 1 \text{ if the } i\text{th fish used the } j\text{th route} \\ (j = \{\mathrm{SUT}, \mathrm{STM}, \mathrm{SAC}\}) \\ 0, \text{ otherwise.} \end{cases}$$

To model route entrainment probabilities as a function of explanatory variables, we used a generalized linear model's framework with a logit link function measured relative to a baseline category, following the methods of Perry et al. (2015). We used the Sacramento River route (SAC) as the baseline category:

$$g\left(\pi_{ij}\right)=\ln\left(\frac{\pi_{ij}}{\pi_{\mathrm{SAC}}}\right)=\beta_{j0}+\beta_{j1}x_{ij1}+\ldots+\beta_{jp}x_{ijp}=\boldsymbol{\beta}_{ij}'\mathbf{x}_{ij} \quad (2)$$

where x_{ijp} is the pth covariate for the ith fish entering the jth route (j = SUT or STM) and β_{jp} is the slope coefficient for the jth route and pth covariate.

Route entrainment probabilities were expressed as a function of covariates using the inverse logit function. The likelihood function to be maximized is the product of Equation 2 over all fish (Agresti 2002). This formulation allows $\pi_{i,\mathrm{SUT}}$ and $\pi_{i,\mathrm{STM}}$ to be modeled by a separate set of explanatory variables. The regression coefficients were estimated by maximum likelihood estimation using optimization routines in R (R Core Team 2021).

We considered the following variables as possible covariates in the model:

- day of the year that fish passed the junction (J_{Day}: mean = 81.5, SD = 13.2),
- time of day (D: day = 1 or night = 0 as defined by time of sunset and sunrise),

https://doi.org/10.15447/sfews.2021v19iss2art4

- tide phase (Tide: flood = 0 or ebb = 1),
- discharge entering Steamboat Slough (Q_{STM}: mean = 77 $m^3 s^{-1}$, SD = 46 $m^3 s^{-1}$), Sutter Slough (Q_{SUT}: mean = 91 $m^3 s^{-1}$, SD = 36 $m^3 s^{-1}$), or the Sacramento River below Steamboat Slough (Q_{SAC}: mean = 170 $m^3 s^{-1}$, SD = 143 $m^3 s^{-1}$),
- change in discharge from time t–1 to t in Steamboat Slough (ΔQ_{STM}, mean = –2.0 $m^3 s^{-1}$, SD = 11.6 $m^3 s^{-1}$) or Sutter Slough (ΔQ_{SUT}, mean = –2.6 $m^3 s^{-1}$, SD = 15.9 $m^3 s^{-1}$),
- proportion of discharge entering Steamboat Slough (P_{STM}: mean = 0.165, SD = 0.059), Sutter Slough (P_{SUT}: mean = 0.213, SD = 0.072), or the Sacramento River below Steamboat Slough (P_{SAC}: mean = 0.623, SD = 0.066).

To characterize the hydrodynamic conditions when each fish passed through the river junction, we associated the time of first detection within each route with the nearest 15-minute flow record. However, we excluded fish that arrived at the junction from an upstream location when flows were reversing from the analysis (n = 127, 3.6% of fish detected in the junction). Arrival under such conditions indicated that the tag was likely in a predator such as Striped Bass (*Morone saxatilis*; Romine et al. 2016). We verified all route assignments using information from downstream receivers (Perry et al. 2018).

Reversing tidal flows at this junction complicate calculation of the proportion of flow that entered each channel. When all three channels had downstream flow, we calculated the proportion of flow that entered each route simply as the discharge (Q_j) entering route j divided by the sum of the discharge in each channel just downstream of the junction (Q_{SUT}, Q_{STM}, Q_{SAC}; Table 1). When discharge was negative in a given route, indicating upstream flow, the proportion of flow that entered that route was set to zero. Thus, the proportion of flow that enters each route is more accurately characterized as the proportion of total outflow that enters each route.

Because some flow metrics are inherently correlated (e.g., flow proportions), not all possible explanatory variables can be included within the same model. Therefore, to identify explanatory variables that best predict migration routing, we identified a full model that consisted of flow metrics with correlations that led to low variance inflation factors (VIF). The full model was formed by a set of variables that had VIF values < 5 (Zuur et al. 2009), excluding variables from the model if they increased VIF values to > 5. This criterion led to inclusion of day of year (J_{Day}), time of day (D), Tidal stage (Tide), P_{SAC}, ΔQ_{STM}, and ΔQ_{SUT} in the linear predictors of both $\varpi_{i,SUT}$ and $\varpi_{i,STM}$. In addition, Q_{STM} and P_{STM} was included in the linear predictor of $\pi_{i,STM}$, and Q_{SUT} and P_{SUT} was included in the linear predictor of $\pi_{i,SUT}$.

Although fish routing is influenced by fine-scale hydrodynamic conditions that result from flows entering each channel, the complexity

Table 1 Proportion of flow entering each route was calculated using the equations shown for the corresponding conditions. Negative indicates reversing or upstream flow, and positive indicates downstream flow.

QSUT	QSTM	QSAC	Sutter Proportion	Steamboat Proportion	Sacramento Proportion
+	+	+	Q_{SUT} /(Q_{SUT} + Q_{STM} + Q_{SAC})	Q_{STM} /(Q_{SUT} + Q_{STM} + Q_{SAC})	Q_{SAC} /(Q_{SUT} + Q_{STM} + Q_{SAC})
+	–	–	1	0	0
+	–	+	Q_{SUT} /(Q_{SUT} + Q_{SAC})	0	Q_{SAC} /(Q_{SUT} + Q_{SAC})
–	–	–	0	0	0
–	+	+	0	Q_{STM} /(Q_{STM} + Q_{SAC})	Q_{SAC} /(Q_{STM} + Q_{SAC})
–	+	–	0	1	0
–	–	+	0	0	1

of the tidal dynamics at this junction made it difficult for us to construct an *a priori* suite of reduced candidate models from the full model. Therefore, we used a two-stage model selection process based on Akaike's Information Criterion (AIC) to identify the model structure that best predicted migration routing. In the first stage, we fit all possible main-effects models for one route (256 possible models for each route), holding the model structure for the other route fixed at the full model. Competing main-effects models were considered those within 2 AIC units of the lowest-AIC model (Burnham and Anderson 2002). We selected the "best" model among the competing models as the lowest AIC model with the fewest predictors, which did not always coincide with the overall lowest-AIC model. For the second stage, we constructed a model that included all main effects retained in the best fit model plus all possible two-way interactions, ran all possible models containing the two-way interactions, and selected the best-fitting model using the same process described above. All continuous explanatory variables used in the regression model were standardized by subtracting the mean from each observation and then dividing by the standard deviation.

We assessed goodness of fit both graphically and statistically. We used the Hosmer–Lemeshow goodness-of-fit test to evaluate how well predicted entrainment probabilities fit observed proportions (Hosmer and Lemeshow 2000). For this test, we ordered predicted entrainment probabilities by rank and divided them into deciles. We then compared mean predicted entrainment probability against the observed proportion within each decile. LOESS [locally estimated scatterplot smoothing] curves were fit to observed entrainment data to compare predicted and observed values (Cleveland et al. 1992).

RESULTS

Of the 4,635 fish tagged and released, we included the 3,418 individuals that transited the junction in the analysis. The majority of the fish remained in the Sacramento River ($n = 2{,}510$) and approximately equal numbers moved into Sutter Slough ($n = 480$, 14%) and Steamboat Slough ($n = 428$, 13%). There was no difference in proportion of tag types that arrived at the junction.

Model selection for main effects models resulted in 16 competing models for Sutter Slough and five competing models for Steamboat Slough (Table 1). For Sutter Slough, we selected the model with both Q_{SUT} and P_{SUT}, which was the lowest-AIC model and had the fewest parameters among competing models. For Steamboat Slough, we selected the model with Q_{STM}, P_{STM}, and ΔQ_{SUT}, which had the fewest variables among competing models but the second-lowest AIC (Table 2). For the second stage of model selection, we formed 16 alternative models from the four possible two-way interactions, which yielded three competing models within 2 AIC of the lowest-AIC model. These competing models contained two to four interaction terms, and were favored considerably over the main effects model without interactions (AIC = 5105.06, ΔAIC = 10.15; Table 3). We selected the simplest of these models for inference, which included one interaction term for each route and was the second-ranked AIC model (Table 4). Although variables such as day of year, tidal stage, and diel period appeared in some of the competing models, discharge and the proportion of flow that entered both Steamboat and Sutter sloughs appeared in almost every competing model, providing additional support for retaining these variables (Table 2).

Model fit diagnostics showed good model fit to data, with no systematic deviations between observed and predicted entrainment proportions (Figure 2). In addition, Hosmer–Lemeshow goodness-of-fit tests for each route were not significant (SUT: $\hat{C} = 22.99$, df = 18, $P = 0.191$; STM: $\hat{C} = 19.53$, df = 18, $P = 0.360$; SAC: $\hat{C} = 15.28$, df = 17, $P = 0.575$).

LOESS curves fitted to the observed binary routing data agreed with predicted probabilities for each individual, indicating that the model performed well at predicting the probabilities of route entrainment under the conditions each fish

https://doi.org/10.15447/sfews.2021v19iss2art4

Table 2 Main-effects model selection results for probability of entrainment at the junction of the Sacramento River with Sutter and Steamboat sloughs, showing all competing models within 2 AIC of the lowest AIC model. Model selection for each route was performed using the full main-effects model for the other route. (* = indicates model selected, NLL = negative log-likelihood, AIC = Akaike's information criterion).

Response	Model	Number of parameters	NLL	AIC	ΔAIC
ϖ_{SUT}	$*Q_{SUT} + P_{SUT}$	12	2543.20	5110.4	0.00
	$Q_{SUT} + P_{SUT} + \Delta Q_{STM}$	13	2542.29	5110.58	0.18
	$Q_{SUT} + P_{SUT} + P_{SAC}$	13	2542.31	5110.62	0.22
	$Q_{SUT} + P_{SUT}$ + Tide	13	2542.70	5111.4	1.00
	$Q_{SUT} + P_{SUT} + \Delta Q_{SUT} + \Delta Q_{STM}$	14	2541.78	5111.56	1.16
	$Q_{SUT} + P_{SUT}$ + D + P_{SAC}	14	2541.86	5111.72	1.32
	$Q_{SUT} + P_{SUT}$ + D	13	2542.87	5111.74	1.34
	$Q_{SUT} + P_{SUT} + \Delta Q_{STM}$ + D	14	2541.88	5111.76	1.36
	$Q_{SUT} + P_{SUT} + \Delta Q_{SUT}$ + P_{SAC}	14	2541.94	5111.88	1.48
	$Q_{SUT} + P_{SAC} + \Delta Q_{SUT}$	13	2542.97	5111.94	1.54
	$P_{SAC} + J_{day}$	12	2544.00	5112	1.60
	$Q_{SUT} + P_{SUT} + \Delta Q_{STM} + P_{SAC}$	14	2542.09	5112.18	1.78
	$Q_{SUT} + P_{SUT} + J_{day} + P_{SAC}$	14	2542.09	5112.18	1.78
	$Q_{SUT} + P_{SUT} + J_{day}$	13	2543.14	5112.28	1.88
	$Q_{SUT} + P_{SAC}$	12	2544.18	5112.36	1.96
	$Q_{SUT} + P_{SUT} + \Delta Q_{SUT}$	13	2543.18	5112.36	1.96
ϖ_{STM}	$Q_{STM} + P_{STM} + \Delta Q_{SUT}$ + Tide	14	2541.26	5110.52	0.00
	$*Q_{STM} + P_{STM} + \Delta Q_{SUT}$	13	2542.75	5111.5	0.98
	$Q_{STM} + P_{STM} + J_{day} + \Delta Q_{SUT}$ + Tide	15	2541.11	5112.22	1.70
	$Q_{STM} + P_{STM} + \Delta Q_{SUT}$ + D + Tide	15	2541.18	5112.36	1.84
	$Q_{STM} + \Delta Q_{SUT} + \Delta QS$ + Tide + P_{STM}	15	2541.22	5112.44	1.92

Table 3 Model selection results assessing interaction terms for probability of entrainment at the junction of the Sacramento River with Sutter and Steamboat sloughs, showing all competing models within 2 AIC of the lowest AIC model. Model selection was performed for all possible models containing two-way interactions among the main effects terms. Model 2 was the final selected model (NLL = negative log-likelihood, AIC = Akaike's information criterion).

	Model	Number of parameters	NLL	AIC	ΔAIC
1	$\varpi_{SUT} \sim Q_{SUT} + P_{SUT} + Q_{SUT}*P_{SUT}$ $\varpi_{STM} \sim Q_{STM} + \Delta Q_{SUT} + P_{STM} + Q_{STM}*P_{STM} + P_{STM}*\Delta Q_{SUT}$	10	2537.44	5094.88	0.00
2	$\varpi_{SUT} \sim Q_{SUT} + P_{SUT} + Q_{SUT}*P_{SUT}$ $\varpi_{STM} \sim Q_{STM} + \Delta Q_{SUT} + P_{STM} + Q_{STM}*P_{STM}$	9	2539.12	5096.24	1.36
3	$\varpi_{SUT} \sim Q_{SUT} + P_{SUT} + Q_{SUT}*P_{SUT}$ $\varpi_{STM} \sim Q_{STM} + \Delta Q_{SUT} + P_{STM} + Q_{STM}*\Delta Q_{SUT} + Q_{STM}*P_{STM} + P_{STM}*\Delta Q_{SUT}$	11	2537.42	5096.84	1.96

Table 4 Maximum likelihood estimates for the best fit model relating route probabilities to covariates

Response	Variable	Estimate (SE)
ϖ_{STM}	Intercept	−1.624 (0.509)
	Q_{STM}	1.077 (0.335)
	P_{STM}	−0.728 (2.724)
	ΔQ_{SUT}	0.159 (0.061)
	$Q_{STM} \cdot P_{STM}$	−4.108 (1.767)
ϖ_{STM}	Intercept	−0.964 (0.544)
	Q_{SUT}	0.814 (0.247)
	P_{SUT}	−3.650 (2.668)
	$Q_{SUT} \cdot P_{SUT}$	−3.028 (1.174)

experienced (Figures 3 and 4). As discharge in the main stem of the Sacramento River increases, probability of entrainment into each of the Sutter and Steamboat sloughs increases. Given the linear relationship between discharge in the Sacramento River and discharge in Sutter Slough and Steamboat Slough, it follows that probability of entrainment into both channels increases as discharge within each channel increases (Figure 3). The relationship between proportion of flow that enters a route and the probability of being entrained in that route was positive (Figure 4). As proportion of flow increased in Sutter Slough, entrainment increased, while entrainment in the other two routes decreased.

When entrainment was predicted across varying flows, emergent patterns revealed brief periods when entrainment into Sutter and Steamboat sloughs is very high. This pattern occurs when tide stage transitioned either from positive to negative flow, or from negative to positive flow (Figures 5 and 6).

DISCUSSION

The proportion of fish that enters different channels in the Delta has been measured by numerous studies, beginning with the pioneering work of Erkkila et al. (1950). However, it is important to recognize that each study estimates entrainment over different time-periods, yielding

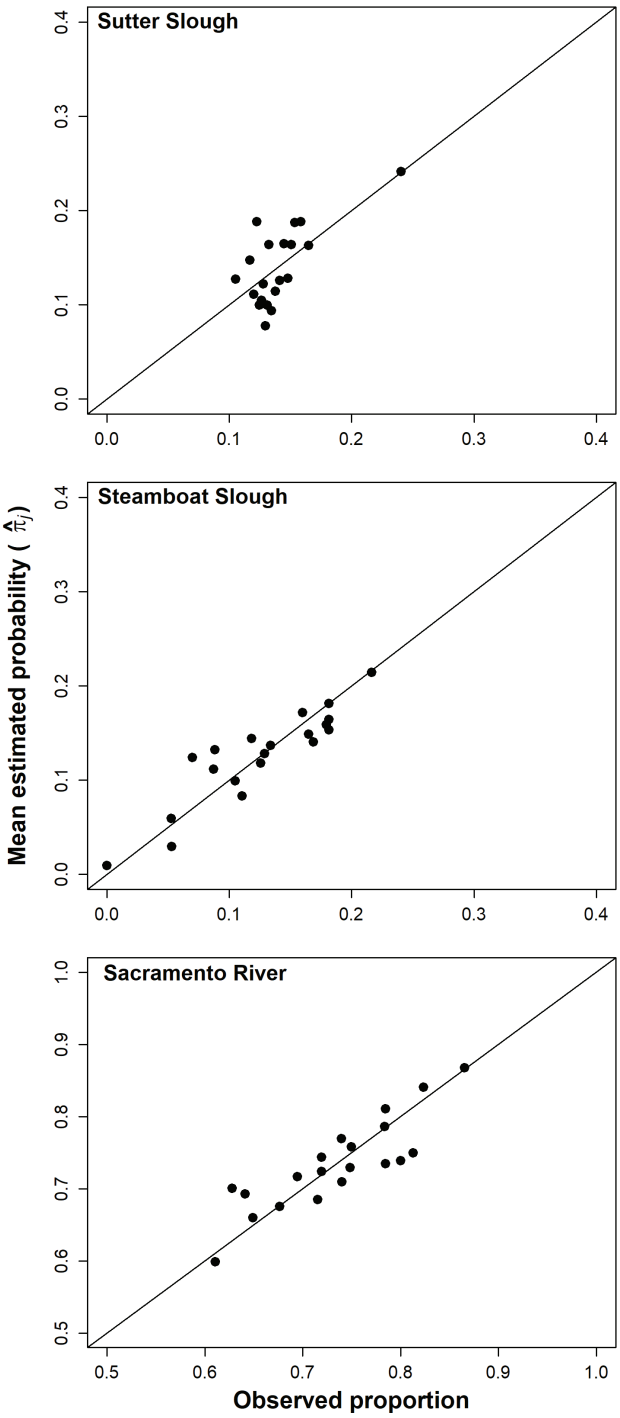

Figure 2 Comparison of observed proportion of fish entrained to each route, and predicted mean probability of entrainment to each route within each decile. The *line* in each plot has a slope of 1 and an intercept of 0. *Points* falling on this line indicate perfect agreement between predicted and observed entrainment rates.

https://doi.org/10.15447/sfews.2021v19iss2art4

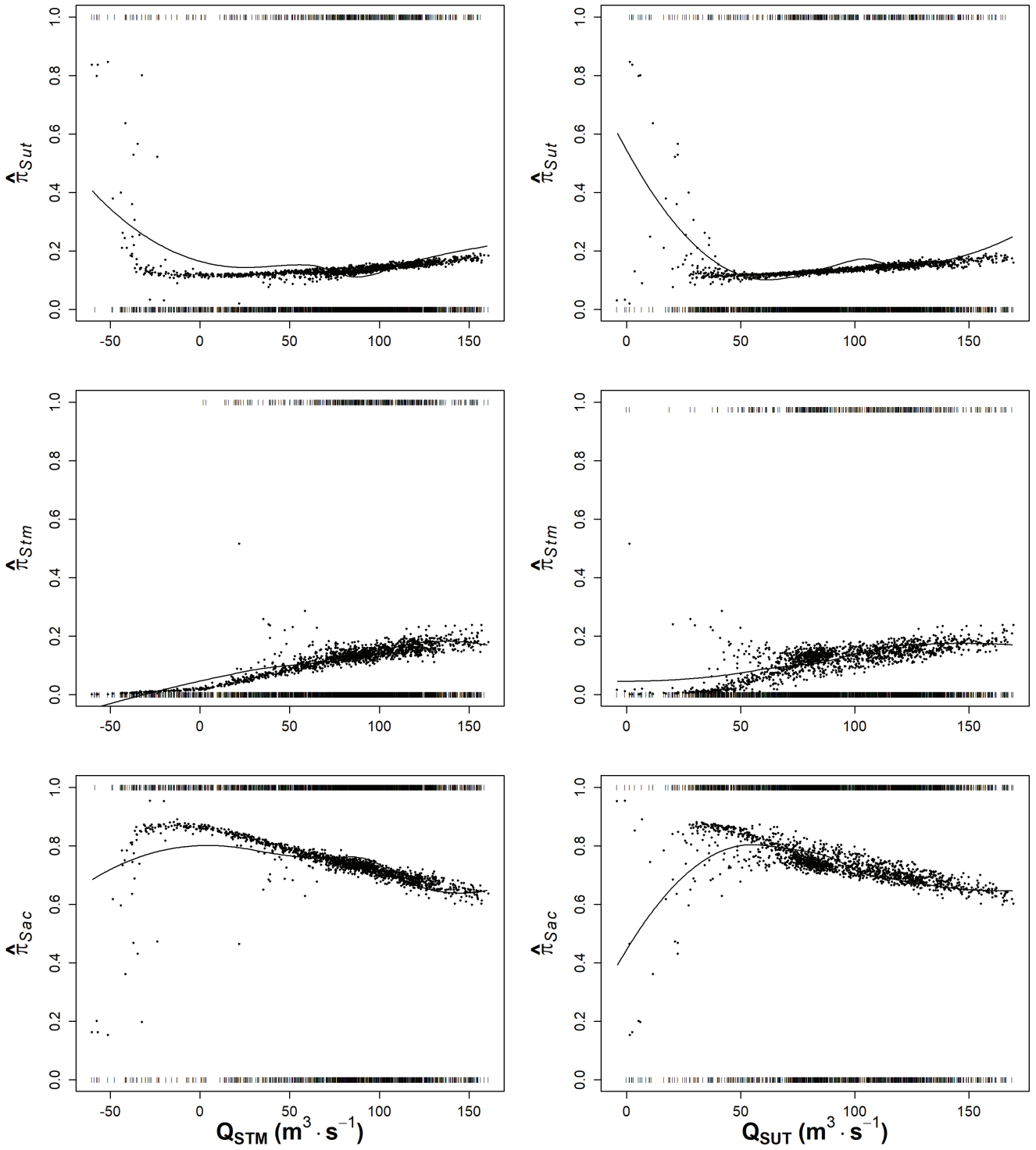

Figure 3 Predicted route entrainment for each fish in each route (circles) as a function of discharge in Steamboat Slough (*left panels*) and Sutter Slough (*right panels*). The *rug plots* indicate the observed entrainment for each fish (0 or 1) and *lines* are LOESS curves fitted to these data. Sac = Sacramento River, Stm = Steamboat Slough, Sut = Sutter Slough, Q = discharge, p = entrainment probability.

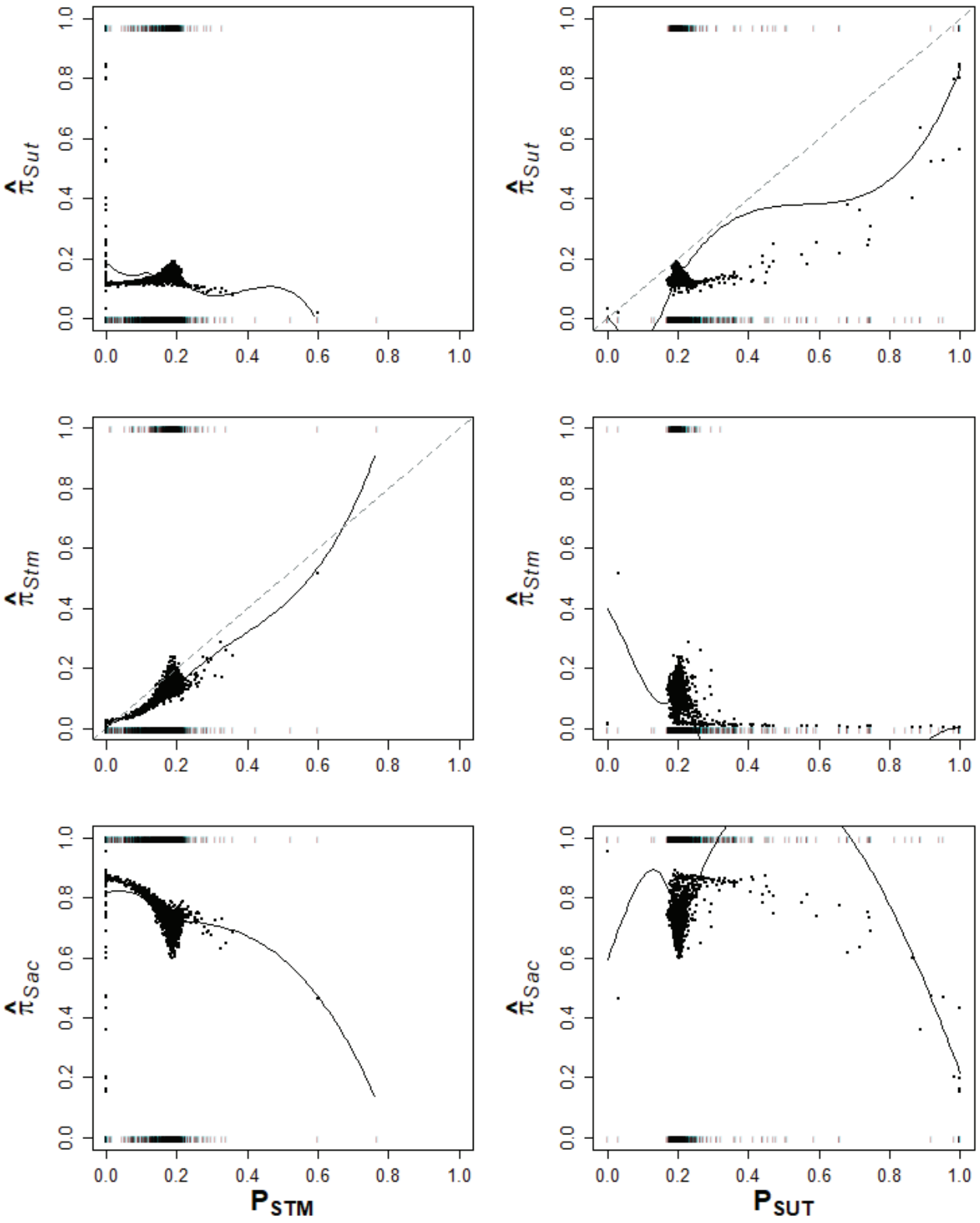

Figure 4 Predicted route entrainment for each fish in each route (*circles*) as a function of proportion of discharge entering Sutter Slough and Steamboat Slough. The *rug plots* indicate the observed entrainment for each fish (0 or 1) and *lines* are LOESS curves fitted to these data. Sac = Sacramento River, Stm = Steamboat Slough, Sut = Sutter Slough, P = proportion of discharge, p = entrainment probability.

https://doi.org/10.15447/sfews.2021v19iss2art4

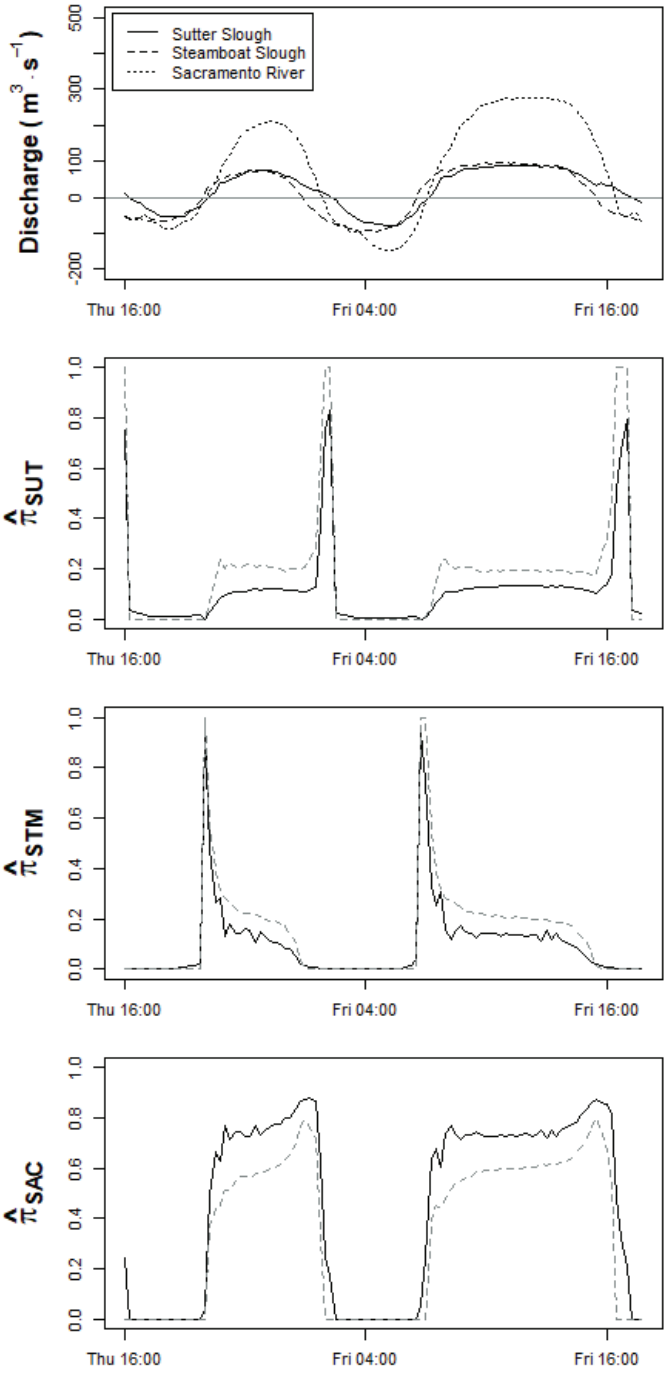

Figure 5 Discharge during the study period (*top panel*) and predicted route entrainment probabilities for Sutter Slough (SUT), Steamboat Slough (STM) and Sacramento River (*solid lines in lower panels*). The figure depicts a period of very low flow between May 15 and May 17, 2014. The *gray dashed line* indicates the proportion of flow entering the route. Sac = Sacramento River, Stm = Steamboat Slough, Sut = Sutter Slough, p = entrainment probability.

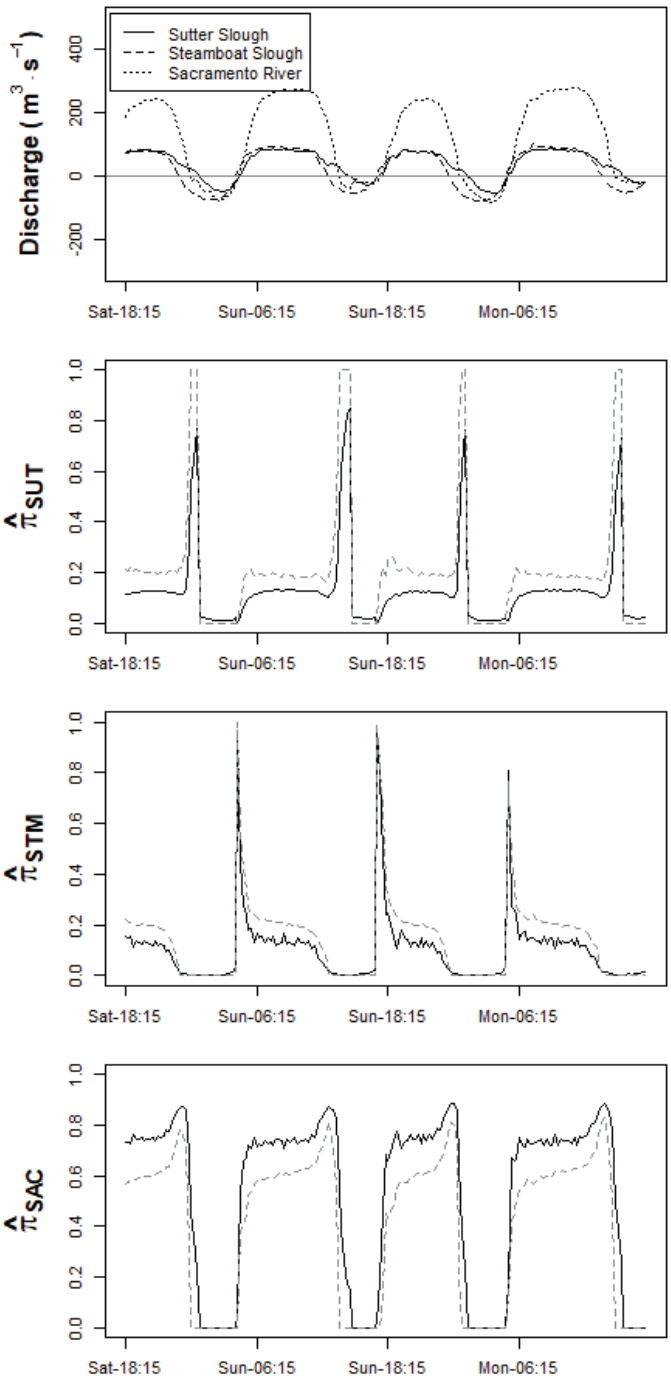

Figure 6 Discharge during the study period (*top panel*) and model predicted route entrainment probabilities for Sutter Slough (SUT), Steamboat Slough (STM) and Sacramento River (*solid line in lower panels*). The figure depicts a period of median flow between April 27 and April 29, 2014. The *gray dashed line* indicates the proportion of flow entering the route. Sac = Sacramento River, Stm = Steamboat Slough, Sut = Sutter Slough, p = entrainment probability.

different types of inferences about the effect of flow variation on fish routing, and the potential consequences of management actions. At the coarsest scale, release-specific (Perry et al. 2010, 2013; Cavallo et al. 2015) or season-wide (Erkkila et al. 1950) estimates represent fish entrainment and flow conditions averaged over multiple days, weeks, or months. These types of entrainment estimates have supported the general hypothesis that fish enter migration routes in proportion to flow. Entrainment estimates at the daily scale provide finer-level information about the effect of net flows on routing, and represent the expected proportion of fish entrained over a given day. Perry et al. (2018) used daily flow covariates to show that the entrainment into Sutter and Steamboat sloughs increased—but entrainment into Georgiana Slough decreased—as tidally averaged flow of the Sacramento River increased.

Although entrainment estimates at daily-to-seasonal temporal scales provide insights into general flow and routing relationships, individual fish pass river junctions over much shorter time-scales (on the order of minutes), and thus are influenced by the particular hydrodynamic conditions that occur when they encounter a channel divergence. At these time-scales, tidal river dynamics can be the dominant factor that determines the hydrodynamic conditions an individual experiences, particularly under low riverine inflows when tidally reversing flows occur. For example, Perry et al. (2015) found that the probability of fish entering Georgiana Slough increased considerably during reverse-flow flood tides, and they identified reverse flows as the primary mechanism that caused the inverse relationship between daily entrainment and net river flow. Thus, quantifying factors that affect routing at tidal time-scales in the Delta is critically important to bridge temporal scales and understand how within-day patterns of entrainment give rise to entrainment integrated over the daily or seasonal scales that are more relevant to population dynamics.

Our results illustrate that the tidal hydrodynamics at this junction are complex, and result in unexpected and temporally variable patterns

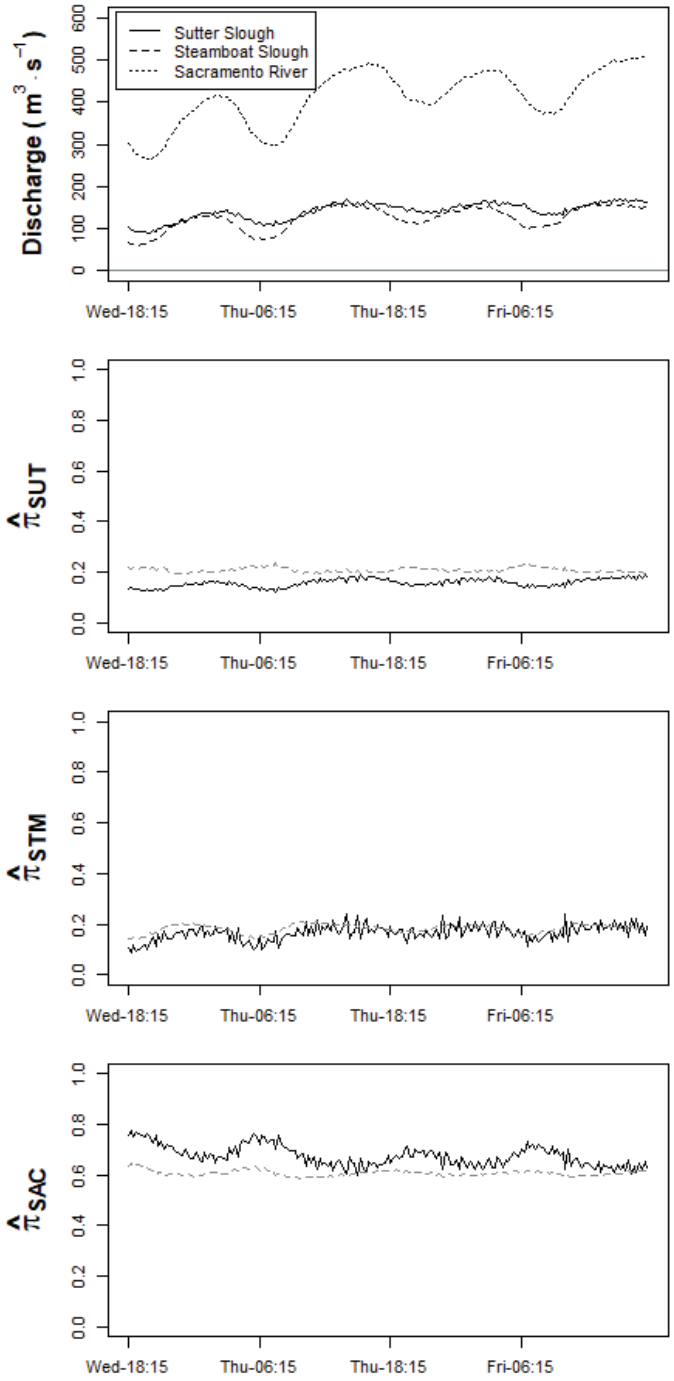

Figure 7 Discharge during the study period (*top panel*) and model predicted route entrainment probabilities for Sutter Slough (SUT), Steamboat Slough (STM) and Sacramento River (*solid line in lower panels*). The figure depicts a period of high flow between March 6 and March 8, 2014. The *gray dashed line* indicates the proportion of flow entering the route. Sac = Sacramento River, Stm = Steamboat Slough, Sut = Sutter Slough, p = entrainment probability.

https://doi.org/10.15447/sfews.2021v19iss2art4

of fish entrainment when flow in the junction transitions from positive or downstream flow to upstream or negative flow (Figures 5 through 7). As Sacramento River discharge decreases and approaches negative flows, we observed a rapid spike in the probability of entrainment into Sutter Slough (Figures 5 and 6). This pattern is likely a result of the fact that flow in Sutter Slough becomes negative after Steamboat Slough and Sacramento River have reversed, thus increasing the proportion of flow into Sutter Slough—and therefore the likelihood that fish would be entrained into this channel up until the point at which flow reverses in Sutter Slough. On the ascending limb of the tide stage, the probability of fish being entrained into Steamboat Slough increases rapidly for a short period of time, which occurs as a result of Steamboat Slough changing from negative flows to positive flows before the other two routes in the junction. Given these observations, time of arrival at the junction has implications for overall entrainment. Fish that arrive at mid ebb and mid flood during low-flow conditions experience a brief period of high entrainment into Sutter Slough and Steamboat Slough, respectively.

Although we identified brief periods of higher entrainment related to flood-tide transitions, the high probability of entrainment did not continue for the duration of the flood tide. This finding contrasts with that of Perry et al. (2015), who found that fish entrainment into Georgiana Slough increased significantly over the entire duration of reverse flows. Flow in Sutter Slough and Steamboat Slough regularly reverses at low inflows, whereas flows in Georgiana Slough and the DCC rarely reverse direction. Thus, fish that have been advected back up the Sacramento River during reverse flows would tend to remain in the Sacramento when flows are simultaneously reversing in Sutter and Steamboat sloughs. In contrast, under the same reverse flow conditions of the Sacramento River, fish can be forced into Georgiana Slough and the DCC (Perry et al. 2015). Our study highlights how factors such as channel geometry, inflow, and tidal forcing interact to produce site-specific hydrodynamic patterns that lead to different entrainment relationships.

In general, we found that the proportion of fish remaining in the Sacramento River was greater than the proportion of flow remaining in the Sacramento River. The opposite pattern occurred for the Sutter and Steamboat sloughs, where there was a lower probability of fish entering each slough relative to the proportion of flow. This is consistent with the findings of Kemp et al. (2005), Perry et al. (2010), and Cavallo et al. (2015); each of these studies found a higher probability of fish remaining in the main channel relative to the proportion of flow. However, at high flows, the proportion of fish that entered Sutter Slough was similar to the proportion of flow that entered Steamboat Slough, indicating that the relationship between proportion of flow and proportion of fish that enter a channel can change with the magnitude of total discharge.

This change in relationship between flow and fish routing is likely related to fish behavior. At higher water velocities, fish can do little to alter their location and actively select a route and are thus constrained by the parcel of water in which they are located, ultimately determining the route they enter (Perry et al. 2016; Hance et al. 2020). Below a threshold of approximately $50\,m^3\,s^{-1}$ ($>0.2\,m^3\,s^{-1}$, ~1.4 body lengths per second), fish may be able to actively cross streamlines to influence their ultimate migration route. This process may explain the increased variation observed in Figure 3. As discharge drops below $50\,m^3\,s^{-1}$ ($0.2\,m^3\,s^{-1}$), fish entrainment becomes more variable with discharge.

CONCLUSION

Our results provide insight into fish entrainment at Sutter and Steamboat sloughs, which may allow managers to consider engineering solutions to increase entrainment into these routes, and thus decrease the proportion of fish that enter the interior Delta (Perry et al. 2014). Although the relationship between flow and entrainment was not directly proportional, entrainment into the sloughs generally increased with an increasing proportion of flow. For managers, this means that as the proportion of flow entering the sloughs increases, the proportion of fish that are

APPENDIX A

Animation of flow entering Sutter Slough and Steamboat Slough (Romine et al. 2021). (Static image is shown below. To view the animation, follow this link: *https://doi.org/10.5066/P9HSLFRE*.)

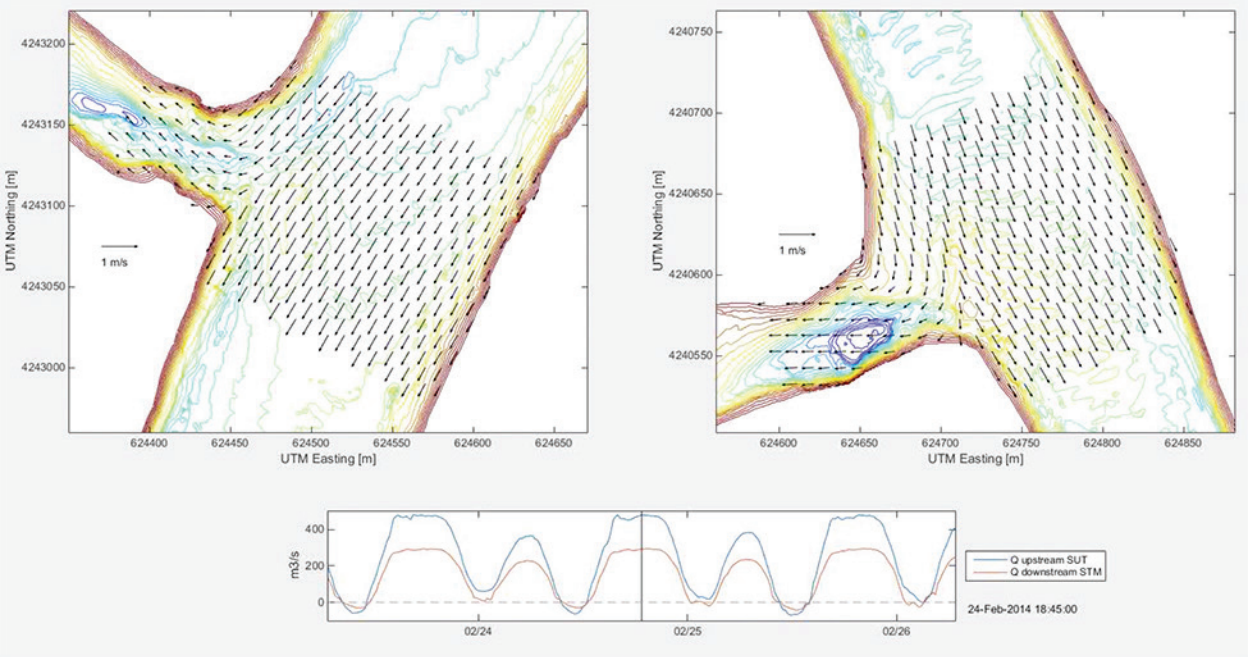

exposed to routes leading to the interior Delta at downstream locations will decrease. Furthermore, by considering how tidal-scale entrainment patterns integrate over longer scales relevant to populations, managers can devise actions that maximize survival across a wide range of inflows and hydrodynamic conditions.

ACKNOWLEDGEMENTS

The authors would like to thank the Delta Stewardship Council for funding that supported this analysis, and the California Department of Water Resources for funding the field work, data collection, and final publication of this manuscript. This project was supported by numerous field personnel of whom there are too many to name here. We are deeply grateful for your hard work and long hours in the field. We would also like to thank Amy Hansen for her editorial assistance. Any use of trade, firm, or product names is for descriptive purposes only and does not imply endorsement by the US Government.

REFERENCES

Agresti A. 2002. Categorical data analysis. Hoboken (NJ): John Wiley and Sons, Inc. 744 p.

Buchanan RA, Skalski JR, Brandes PL, Fuller A. 2013. Route use and survival of juvenile Chinook Salmon through the San Joaquin River Delta. N Am J Fish Manag. [accessed 2021 Apr 1];33:216–229. *https://doi.org/10.1080/02755947.2012.728178*

Burnham KP, Anderson DR. 2002. Model selection and multimodel inference: A practical information-theoretic approach. 2nd ed. New York (NY): Springer.

Cavallo B, Gaskill P, Melgo J, Zeug SC. 2015. Predicting juvenile Chinook salmon routing in riverine and tidal channels of a freshwater estuary. Env Biol Fish. [accessed 2021 April 01];98:1571–1582. *https://doi.org/10.1007/s10641-015-0383-7*

Cleveland, WS, Grosse, E, and Shyu, WM. 1992. In: Chambers JM, Hastie TJ, editors. Statistical models in S. Boca Raton (FL): Wadsworth & Brooks/Cole. p. 201–309.

Erkkila, LF, Moffett, JW, Cope, OB, Smith, BR and Nelson, RS. 1950. Sacramento–San Joaquin Delta fishery resources: effects of Tracy Pumping Plant and Delta Cross Channel. US Fish and Wildlife Service Special Scientific Report 56. 109 p.

Hance DJ, Perry RW, Burau JR, Blake A, Stumpner P, Wang X, Pope A. 2020. Combining models of the critical streakline and the cross-sectional distribution of juvenile salmon to predict fish routing at river junctions. San Franc Estuary Watershed Sci. [accessed 2021 April 01];18(1). *https://doi.org/10.15447/sfews.2020v18iss1art3*

Hosmer DW, Lemeshow S. 2000. Applied Logistic Regression. Hoboken (NJ): John Wiley & Sons, Inc. 383 p.

Kemp PS, Gessel MH, Williams JG. 2005. Fine-scale behavioral responses of Pacific salmonid smolts as they encounter divergence and acceleration of flow. Trans Am Fish Soc. [accessed 2021 April 01]; 134:390–398. *https://doi.org/10.1577/T04-039.1*

Liedtke TL, Beeman JW, Gee LP. 2012. A standard operating procedure for the surgical implantation of transmitters in juvenile salmonids. US Geological Survey Open-File Report 2012-1267. [accessed 2021 April 01]. 50 p. Available from: *http://pubs.usgs.gov/of/2012/1267*

Liedtke TL, Wargo-Rub MA. 2012. Techniques for telemetry transmitter attachment and evaluation of transmitter effects on fish performance. In: Adams NS, Beeman JW, Eiler JW, editors. 2012. Telemetry techniques: a user's guide for fisheries research. Bethesda (MD): American Fisheries Society. p. 45–87.

Lindley ST, Grimes CB, Mohr MS, Peterson W, Stein J, Anderson JT, Botsford LW, Bottom DL, Busack CA, Collier TK, et al. 2009. What caused the Sacramento River fall Chinook stock collapse? US Department of Commerce, NOAA Technical Memorandum. NOAA-TM-NMFS-SWFSC-447. [accessed 2021 April 01]; 61 p. Available from: *https://repository.library.noaa.gov/view/noaa/3664/noaa_3664_DS1.pdf*

[NMFS] National Marine Fisheries Service. 2014. Recovery plan for evolutionarily significant units of Sacramento River winter-run Chinook Salmon and Central Valley spring-run Chinook Salmon and the distinct population segment of California Central Valley Steelhead. California Central Valley Area Office. [accessed 2021 Apr 01]. 1561 p. Available from: *https://media.fisheries.noaa.gov/dam-migration/central_valley_salmonids_recovery_plan-accessible.pdf*

Newman KB, Brandes PL. 2010. Hierarchical modeling of juvenile Chinook Salmon survival as a function of Sacramento–San Joaquin Delta water exports. N Am J Fish Manag. [accessed 2021 April 01];30:157–169. *https://doi.org/10.1577/M07-188.1*

Nichols FH, Cloern JE, Luoma SN, Peterson DH. 1986. The modification of an estuary. Science. [accessed 2021 April 01];231:567–573. *https://doi.org/10.1126/science.231.4738.567*

Perry RW, Brandes PL, Burau JR, Klimley AP, MacFarlane B, Michel C, Skalski JR. 2013. Sensitivity of survival to migration routes used by juvenile Chinook Salmon to negotiate the Sacramento–San Joaquin River Delta. Env Biol Fish. [accessed 2021 April 01];96:381–392. *https://doi.org/10.1007/s10641-012-9984-6*

Perry RW, Brandes PL, Burau JR, Sandstrom PT, Skalski JR. 2015. Effect of tides, river flow, and gate operations on entrainment of juvenile Salmon into the interior Sacramento–San Joaquin River Delta. Trans Am Fish Soc. [accessed 2021 April 01];144:445–455. *https://doi.org/10.1080/00028487.2014.1001038*

Perry RW, Buchanan RA, Brandes PL, Burau JR, and Israel JA. 2016. Anadromous salmonids in the Delta: new science 2006–2016. San Franc Estuary Watershed Sci. [accessed 2021 April 01];14(2). *https://doi.org/10.15447/sfews.2016v14iss2art7*

Perry RW, Pope AC, Romine JG, Brandes PL, Burau JR, Blake AR, Amman AJ and Michel CJ. 2018. Flow-mediated effects on travel time and survival of juvenile Chinook Salmon vary spatially in a complex tidally forced river delta. Can J of Fish Aquat Sci. [accessed 2021 April 01];75:1886–1901. *https://doi.org/10.1139/cjfas-2017-0310*

Perry RW, Romine JG, Adams NS, Blake AR, Burau JR, Johnston SV, Liedtke TL. 2014. Using a non-physical behavioural barrier to alter migration routing of juvenile Chinook Salmon in the Sacramento–San Joaquin River Delta. Riv Res Appl. [accessed 2021 April 01];30:192–203. *https://doi.org/10.1002/rra.2628*

Perry RW, Skalski JR, Brandes PL, Sandstrom PT, Klimley AP, Ammann A, MacFarlane RB. 2010. Estimating survival and migration route probabilities of juvenile Chinook Salmon in the Sacramento–San Joaquin River Delta. N Am J Fish Manag. [accessed 2021 April 01];30:142–156. *https://doi.org/10.1577/M08-200.1*

Plumb JM, Adams NS, Perry RW, Holbrook CM, Romine JG, Blake AR, Burau JR. 2016. Diel activity patterns of juvenile late fall run Chinook Salmon with implications for operation of a gated water diversion in the Sacramento–San Joaquin River Delta. Riv Res Appl. [accessed 2021 April 01];32:711–720. *https://doi.org/10.1002/rra.2628*

R Core Team. 2021. R: a language and environment for statistical computing. Vienna (Austria): R Foundation for Statistical Computing. [accessed 2021 April 01]. Available from: *http://www.R-project.org/*

Romine JG, Perry RW, Pope AC, Stumpner P, Liedtke TL, Kumagai KK, Reeves RL. 2016. Evaluation of a floating fish guidance structure at a hydrodynamically complex divergence in the Sacramento–San Joaquin River Delta, California, US Mar Fresh Res. [accessed 2021 April 01];68:878–888. *https://doi.org/10.1071/MF15285*

Romine JG, Perry RW, Stumpner PR, Blake AR, Burau JR. 2021. Tidal flow dynamics at Sutter and Steamboat Sloughs in the Sacramento-San Joaquin Delta, CA. 2014 US Geological Survey data release. [Accessed 2021 June 06]. *https://doi.org/10.5066/P9HSLFRE*

Ruhl CA, Simpson MR. 2005. Computation of discharge using the index-velocity method in tidally affected areas. Sacramento (CA): U.S. Geological Survey Scientific Investigations Report 2005-5004. [accessed 2021 April 01]. 31 p. Available from: *https://pubs.er.usgs.gov/publication/sir20055004*

[SJRG] San Joaquin River Group Authority 2013. 2011 Annual Technical Report—On Implementation and monitoring of the San Joaquin River Agreement and the Vernalis Adaptive Management Plan (VAMP). Davis (CA): San Joaquin River Group Authority. [accessed 2021 April 01]. 339 p.

Zuur AF, Ieno E, Walker, NJ, Saveliev AA, Smith G. 2009. Mixed effects models and extensions in ecology with R. New York (NY): Springer. 574 p.

https://doi.org/10.15447/sfews.2021v19iss2art4